*Anal. Chem.* **2003,** *75,* 2678−2687

# Boron-Doped Diamond Microelectrodes for Use in Capillary Electrophoresis with Electrochemical Detection

Josef Cvačka,[†] Veronika Quaiserová,[‡] JinWoo Park,[†] Yoshiyuki Show,[†] Alexander Muck, Jr.,[‡] and Greg M. Swain*[,†]

*Department of Chemistry, 320 Chemistry Building, Michigan State University, East Lansing, Michigan 48824-1322, and UNESCO Laboratory of Environmental Electrochemistry, Department of Analytical Chemistry, Charles University, Hlavova 2030/8, 128 43 Prague, Czech Republic*

**The fabrication and characterization of boron-doped diamond microelectrodes for use in electrochemical detection coupled with capillary electrophoresis (CE−EC) is discussed. The microelectrodes were prepared by coating thin films of polycrystalline diamond on electrochemically sharpened platinum wires (76-, 25-, and 10-$\mu$m diameter), using microwave-assisted chemical vapor deposition (CVD). The diamond-coated wires were attached to copper wires (current collectors), and several methods were explored to insulate the cylindrical portion of the electrode: nail polish, epoxy, polyimide, and polypropylene coatings. The microelectrodes were characterized by scanning electron microscopy, Raman spectroscopy, and cyclic voltammetry. They exhibited low and stable background currents and sigmoidally shaped voltammetric curves for $Ru(NH_3)_6^{3+/2+}$ and $Fe(CN)_6^{3-/4-}$ at low scan rates. The microelectrodes formed with the large diameter Pt and sealed in polypropylene pipet tips were employed for end-column detection in CE. Evaluation of the CE−EC system and the electrode performance were accomplished using a 10 mM phosphate buffer, pH 6.0, run buffer, and a 30-cm-long fused-silica capillary (75-$\mu$m i.d.) with dopamine, catechol, and ascorbic acid serving as test analytes. The background current (∼100 pA) and noise (∼3 pA) were measured at different detection potentials and found to be very stable with time. Reproducible separation (elution time) and detection (peak current or area) of dopamine, catecho,l and ascorbic acid were observed with response precisions of 4.1% or less. Calibration curves constructed from the peak area were linear over 4 orders of magnitude, up to a concentration between 0.1 and 1 mM. Mass limits of detection for dopamine and catechol were 1.7 and 2.6 fmol, respectively (S/N = 3). The separation efficiency was ∼33 000, 56 000, and 98 000 plates/m for dopamine, catechol, and ascorbic acid, respectively. In addition, the separation and detection of 1- and 2-naphthol in 160 mM borate buffer, pH 9.2, was investigated. Separation of these two analytes was achieved with efficiencies of 118 000 and 126 000 plates/m, respectively.**

Capillary electrophoresis (CE) is a powerful separation technique, in both the classical column and microchip formats.[1] The technique provides high separation efficiency, short analysis times, and low sample consumption. Several detection methods have been coupled with CE, absorption and fluorescence spectroscopy, electrochemistry, and more recently, mass spectrometry. Reviews covering the various detection methods have appeared in the literature.[2−4] Some of the advantages of electrochemical detection (EC) are high sensitivity, which is not compromised by the miniaturization, and rather simple and inexpensive instrumentation.[5−7] Besides the challenges associated with decoupling the separation voltage from the electrode response and alignment of the working electrode at the end of the separation capillary, the major issues with electrochemical detection (e.g., amperometric) are electrode fouling and the need for frequent electrode pretreatment. Nearly all carbon electrodes, including carbon fibers, are susceptible to strong adsorption of polar aromatic analytes, reaction intermediates, reaction products, or other contaminants, and can easily be deactivated, requiring some form of pretreatment to renew the surface. Additionally, at the positive potentials used for oxidative detection of many analytes, the carbon fiber surface microstructure and chemistry can change dynamically over time as a result of surface oxidation processes. Over time, this leads to increased and often unstable background currents.

Recently, a new carbon electrode material, boron-doped diamond, has begun to be studied.[8−10] Polycrystalline, boron-doped

[†] Michigan State University.
[‡] Charles University.

(1) El Rassi, Z., Ed. *CE and CEC Reviews 2002: Advances in the Practice and Application of Capillary Electrophoresis and Capillary Electrochromatography*; John Wiley & Sons: New York, 2002.
(2) Swinney, K.; Bornhop, D. J. *Electrophoresis* **2000**, *21*, 1239.
(3) Matysik, F.-M. *Electrophoresis* **2002**, *23*, 400.
(4) Baldwin, R. P. *Electrophoresis* **2000**, *21*, 4017.
(5) Ewing, A. G.; Wallingford, R. A.; Olefirowicz, T. M. *Anal. Chem*. **1989**, *61*, 292A.
(6) Lacher, N. A.; Garrison, K. E.; Martin, R. S.; Lunte, S. M. *Electrophoresis* **2001**, *22*, 2526.
(7) Zhong, M.; Zhou, J.; Lunte, S. M.; Zhao, G.; Giolando, D. M.; Kirchhoff, J. R. *Anal. Chem*. **1996**, *68*, 203.
(8) Granger, M. C.; Witek, M.; Xu, J.; Wang, J.; Hupert, M.; Hanks, A.; Koppang, M. D.; Butler, J. E.; Lucazeau, G.; Mermoux, M.; Strojek, J. W.; Swain, G. M. *Anal. Chem*. **2000**, *72*, 3793.



10.1021/ac030024z CCC: $25.00 © 2003 American Chemical Society
Published on Web 04/30/2003

diamond thin-film electrodes possess excellent electrochemical properties, such as a low and stable background current over a wide potential range; superb microstructural stability at extreme cathodic and anodic potentials and high current densities; good responsiveness for many redox analytes without pretreatment; and resistance to fouling because of weak adsorption of polar analytes on the low-oxygen, hydrogen-terminated surface. Planar thin-film electrodes, in a macro-sized architecture, have been the most studied form of the electrode, thus far. Although planar electrodes are well-suited for many electroanalytical applications, their dimensions are inappropriate for detection in small volumes (e.g., electrochemical detection with CE) or when a high level of spatial resolution is needed.

Diamond microelectrodes may offer superior analytical figures of merit, as compared to carbon fibers and metal wires, in terms of linear dynamic range, limit of detection, response precision, and stability. Several approaches can be used to fabricate diamond microelectrodes: (i) conformal diamond coatings on small-diameter wires, (ii) coatings on the end of capillary columns, (iii) deposition of diamond on lithographically patterned substrates, and (iv) oxygen-based ion beam plasma etching of bulk diamond material. To the best of our knowledge, the latter two approaches have not yet been used for the fabrication of individual boron-doped diamond microelectrodes. However, lithographic techniques have been used to fabricate diamond disk microelectrode arrays.[11] There are a few reports describing electrochemical investigations of diamond microelectrodes. Cooper et al. reported on the deposition of boron-doped diamond on etched tungsten wires (250 $\mu$m diameter).[12] Either single microcrystallites grown on the end of the wire or continuous diamond films deposited over the entire wire were prepared and sealed in glass to construct the microelectrode. Electrodes with radii between 3 and 7 $\mu$m were produced by careful polishing and etching of the glass in HF. Sarada et al. reported on the electrochemical response of boron-doped diamond films deposited on etched tungsten wires (50-$\mu$m diameter).[13] The microdisk electrodes were prepared by sealing the wires in glass tubes using a low-viscosity epoxy, followed by mechanical polishing to expose the diamond surface. In both reports, difficulties with the reproducibility of fabricating the microelectrodes were mentioned. More recently, Martin and co-workers have been very active in the development of diamond microelectrodes for use in bioanalysis.[14] Publications by Shin et al. and Wang et al. describing the use of diamond microelectrodes for electrochemical detection in both column and microchip capillary electrophoresis have also recently appeared.[15,16]

There are two important practical issues associated with the fabrication of diamond microelectrodes: the reproducible deposition of highly conducting and conformal diamond films on fiberous substrates and developing a simple and reliable method for insulating the cylindrical portion of the microelectrode. Diamond microelectrodes cannot easily be sealed in glass due to the rough polycrystalline film and the difference in thermal expansion coefficient of the two materials. In addition, the sealed electrodes cannot be cut and polished to expose a well-defined disk geometry, as can carbon fibers. Several methods have been reported for insulating microelectrodes, for example, platinum microelectrodes for scanning tunneling microscopy, including glass,[17,18] poly($\alpha$-methylstyrene),[17,18] polyimide,[19] and various electrophoretic paints.[20−22] Etched carbon fibers have also been sealed with poly(oxyphenylene).[23] These methods may very well be useful for diamond. The challenge is to develop a coating method for diamond that will reproducibly seal the cylindrical portion of the microelectrode and allow exposure of a well-defined disk geometry.

We report on the fabrication and characterization of the diamond microelectrodes formed on sharpened platinum wires, the basic electrochemical properties of such electrodes, and their use in electrochemical detection coupled with CE. The objectives of the work were (i) to demonstrate the fabrication of microelectrodes by depositing polycrystalline diamond on sharpened platinum wires, (ii) to characterize these electrodes and evaluate their electrochemical responsiveness, (iii) to evaluate coating procedures for their ability to insulate the cylindrical portion of the microelectrode, and (iv) to test the electrode performance in CE−EC. Boron-doped polycrystalline diamond thin films were deposited on platinum wires (10-, 25-, and 76-$\mu$m diameter) that were first electrochemically sharpened and ultrasonically seeded in a diamond particle suspension to enhance nucleation. Platinum has several properties that make it a suitable substrate. First, it can be easily etched into high-aspect ratio shape, and its melting temperature is high (1768 °C) so that no shape deformation occurs during diamond deposition (~800 °C). Second, it can be deposited and patterned on insulating substrates, such as quartz, creating the possibility of fabricating diamond microelectrode arrays. Third, the characteristic voltammetric features of the metal could be used as an indicator of cracks and pinholes in the diamond film, if they were to exist. The diamond-coated wires were attached to copper wires using silver epoxy and were insulated by one of four methods: nail polish, epoxy, polyimide, or polypropylene coatings. The microelectrodes were characterized using scanning electron microscopy (SEM), Raman spectroscopy, and cyclic voltammetry. The 76-$\mu$m-diameter microelectrodes were sealed in polypropylene pipet tips and employed in end-column electrochemical detection with CE. The electrophoretic separation and amperometric detection of (i) dopamine, catechol, and ascorbic acid, and (ii) 1- and 2-naphthol are discussed.


(9) Xu, J.; Granger, M. C.; Chen, Q.; Strojek, J. W.; Lister, T. E.; Swain, G. M. *Anal. Chem*. **1997**, *69*, 591A.
(10) Granger, M. C.; Xu, J.; Strojek, J. W.; Swain, G. M. *Anal. Chim. Acta* **1999**, *397*, 145.
(11) Tsunozaki, K.; Einaga, Y.; Rao, T. N.; Fujishima, A. *Chem. Lett*. **2002**, 502.
(12) Cooper, J. B.; Pang, S.; Albin, S.; Zheng, J.; Johnson, R. M. *Anal. Chem*. **1998**, *70*, 464.
(13) Sarada, B. V.; Rao, T. N.; Tryk, D. A.; Fujishima, A. *J. Electrochem. Soc*. **1999**, *146*, 1469.
(14) Martin, H. B.; Angus, J. C.; Wightman, R. M. *Pittcon 2002*; Abstract no. 1046.
(15) Shin, D.; Sarada, B. V.; Tryk, D. A.; Fujishima, A.; Wang, J. *Anal. Chem*. **2003**, *75*, 530.
(16) Wang, J.; Chen, G.; Chatrathi, M. P.; Fujishima, A.; Tryk, D. A.; Shin, D. *Anal. Chem*. **2003**, *75*, 935.
(17) Heben, M. J.; Dovek, M. M.; Lewis, N. S.; Penner, R. M.; Quate, C. F. *J. Microsc*. **1988**, *152*, 651.
(18) Penner, R. M.; Heben, M. J.; Lewis, N. S. *Anal. Chem*. **1989**, *61*, 1630.
(19) Sun, P.; Zhang, Z.; Guo, J.; Shao, Y. *Anal. Chem*. **2001**, *73*, 5346.
(20) Bach, C. E.; Nichols, R. J.; Beckmann, W.; Meyer, H.; Schulte, A.; Besenhard, J. O.; Jannakoudakis, P. D. *J. Electrochem. Soc*. **1993**, *140*, 1281.
(21) Slevin, C. J.; Gray, N. J.; Macpherson, J. V.; Webb, M. A.; Unwin, P. R. *Electrochem. Commun*. **1999**, *1*, 282.
(22) Conyers, J. L., Jr.; White, H. S. *Anal. Chem*. **2000**, *72*, 4441.
(23) Kawagoe, K. T.; Jankowski, J. A.; Wightman, R. M. *Anal. Chem*. **1991**, *63*, 1589.

## EXPERIMENTAL SECTION

**Materials and Chemicals.** Platinum wire was obtained from Aldrich (St. Louis, MO, 76-$\mu$m diameter, 99.99% pure) and Goodfellow Cambridge Ltd. (Huntingdon, England, 25-$\mu$m diameter, 99.99% pure; and 10-$\mu$m diameter, 99.9% pure). All chemicals were reagent-grade quality or better and were used without additional purification. The chemicals used for electrode performance testing were hexaammineruthenium(III) chloride, potassium ferrocyanide (II) trihydrate, catechol, 4-*tert*-butylcatechol, 4-methylcatechol, epinephrine, (±)-norepinephrine L-bitartrate hydrate, and 3-hydroxytyramine hydrochloride (dopamine) (Aldrich), and L-ascorbic acid and 3,4-dihydroxyphenylacetic acid (DOPAC) (Sigma, St. Louis, MO). The 1- and 2-naphthol were used without additional purification (Aldrich). The reagents used for the polyimide coating, 4,4′-oxydianiline (97%), 1,2,4,5-benzenetetracarboxylic dianhydride, and *N*,*N*-dimethylacetamide (HPLC grade), were purchased from Aldrich. Reagent-grade calcium chloride dihydrate was purchased from Fisher Scientific (Pittsburgh, PA), and acetone (ACS grade) was obtained from Columbus Chemical Industries (Columbus, WI). The chemicals used for the preparation of the buffers and supporting electrolytes, potassium phosphate monobasic, potassium phosphate dibasic, and potassium chloride, were purchased from Spectrum Chemical (Gardena, CA). The sodium tetraborate ($Na_2B_4O_7 \cdot 10H_2O$) was purchased from Aldrich. Perchloric acid (99.999%) was obtained from Aldrich. The nail polish (Naturistics Super Shine Crystal Clear) was purchased from Del Laboratories (Famingdale, NY), and Quick Setting Epoxy Adhesive, from PACER Technology (Rancho Cucamonga, CA). Ultrapure 18 MΩ water (Barnestead E-Pure System) was used for all solution preparation and for the glassware and electrode cleaning.

**Platinum Etching Procedure.** The etching solution was prepared by dissolving 7.00 g of $CaCl_2 \cdot 2H_2O$ in a mixture of 20 mL of ultrapure water and 20 mL of acetone.[24] The solution was allowed to stand overnight for complete mixing. The etching apparatus consisted of a small Teflon vessel equipped with four equidistantly spaced carbon rod electrodes electrically connected together. A 2-cm piece of 76-$\mu$m platinum wire, designated for sharpening, was cut and bent in the middle so that both ends could be immersed into the solution at the same time. The distance between ends was 2−3 mm. The center of the platinum wire was attached to a holder, fabricated from a small alligator clip soldered to thick copper wire. Both wire ends were immersed to a depth of 1 to 2 mm in the center of the four carbon rods. A sinusoidal polarization of 12 V was applied between the holder and carbon rod counter electrodes using a variable autotransformer (Staco Energy Products, Dayton, OH). The etching procedure was considered complete after ∼45 s, a point at which obvious gas evolution ceased. The etched platinum wire was then thoroughly cleaned with a stream of water, bent back into a straight shape, and allowed to dry. The smaller diameter platinum wires were electrochemically sharpened in a similar manner, except that each was etched one end at a time. The 10- and 25-$\mu$m-diameter wires were electrochemically etched using 3.0 and 3.5 V, respectively, and the procedure was considered complete in 10 and 20 s.

(24) Libioulle, L.; Houbion, Y.; Gilles, J.-M. *Rev. Sci. Instrum.* **1995**, *66*, 97.

**Diamond Film Deposition.** Boron-doped diamond thin films were deposited on the sharpened wires, using microwave-assisted CVD (1.5 kW, 2.54 GHz, ASTeX, Woburn, MA). Prior to deposition, the wires were ultrasonically cleaned in acetone (5−10 min.) and "seeded" in a diamond powder suspension (5-nm particles, ∼20 mg in 100 mL of ethanol, Tomai Diamond Co., Tokyo, Japan) for 30 min. To prevent damage to the sharpened ends, each wire was sonicated separately while suspended in the solution, using a special holder rather than resting against the bottom of the glass container. During the seeding process, the surface was scratched and some residual diamond particles were embedded. Both sites served as nucleation centers during film growth. The platinum wires (3−4 in number) were mounted in parallel fashion on top of a quartz plate (10 × 10 × 1 mm) in the reactor. The quartz plate rested in the center of the molybdenum substrate stage and served to thermally isolate the wires. The 25- and 10-$\mu$m-diameter wires, because of their low mass, were secured into position using photoresist (Microposit S1818, Shipley Company, Marlborough, MA), and the weight of two additional platinum wires was placed orthogonally across their top. This was necessary to keep the wires from moving during pump-down and plasma turn-on.The photoresist quickly gasifies during the initial phase of the growth and does not influence the film quality. Boron-doped diamond films were deposited from a 0.5% $CH_4/H_2$ source gas mixture with doping accomplished using a solid-state diffusion source (Boron Plus GS-126, Techneglas, Perrysburg, OH). The source was placed on the molybdenum stage adjacent to the wires. More recently, we have incorporated a gas-phase dopant source, $B_2H_6$ diluted in $H_2$. The plasma was formed with all the ultrahigh purity (>99.998%) gases flowing into the reactor. The microwave power was 800 W, the system pressure was 35 Torr, the substrate temperature was ∼800 °C (estimated with an optical pyrometer), and the total gas flow was ∼200 sccm. The deposition time was 10.5 h. During the first 30 min of deposition, an elevated 3.5% $CH_4/H_2$ source-gas ratio (high carbon concentration) was used to enhance the nucleation density.

**Film Characterization.** Scanning electron microscopy was performed with either a JEOL 6400V electron microscope equipped with $LaB_6$ emitter or a JEOL 6300F with field-emission microscope (both JEOL, Tokyo, Japan). The samples were attached to a specimen stub using double-sided carbon adhesive tape. The insulated microelectrodes (nail polish, polyimide, or polypropylene) were sputter-coated with a thin layer of gold to reduce surface charging by the electron beam. An accelerating voltage of 15 kV and a 15-mm working distance were used for imaging. Images were recorded digitally using analySIS software (Soft Imaging System, Münster, Germany). Raman spectra were obtained using Raman 2000 instrument (Chromex, Albuquerque, NM) equipped with a 50-mW Nd:YAG laser (532 nm line). Spectra were acquired using a 3-$\mu$m spot size with an integration time of 10 s. The spectrometer was calibrated (wavelength position) with 4-acetamidophenol ($CH_3CONHC_6H_4OH$).

**Microelectrode Construction.** The diamond-coated platinum wire was placed on Teflon tape and cut in half above the area coated with diamond. A copper wire (10-cm length, 0.3-mm diameter) was then attached, using conductive silver epoxy CW2400 (Chemtronics, Kennesaw, GA). The epoxy was cured overnight at room temperature. Several methods were investigated

for insulating the cylindrical portion of the wire. One method utilized nail polish or epoxy. Both of these coatings were applied with a small brush and were allowed to cure for several hours at room temperature. Microelectrodes with less exposed area were sealed with a polyimide film. The coating solution was prepared by dissolving of 0.525 g of 4,4′-oxydianiline and 0.572 g of 1,2,4,5-benzenetetracarboxylic dianhydride in 8.0 mL of *N*,*N*-dimethylacetamide.[18] The microelectrode was dipped into the coating solution and cured vertically for 10 min at 180 °C in an oven. This process was repeated several times. Excess solution was removed each time by a stream of nitrogen gas. The coating progress was monitored by measuring cyclic voltamograms in 1 M KCl. The microelectrodes were completely insulated (negligible current flow) after 5−10 coating cycles. The end of the diamond electrode was then exposed by dissolving the polymer film in sodium hydroxide. The electrode was first wrapped in Teflon tape, with only the electrode end exposed. The electrode was then placed in contact with a Kimwipe (Kimberly-Clark Corporation, Roswell, GA) saturated in 0.1 M NaOH for 1 to 60 min. The alkaline solution dissolved the polymer, exposing the diamond electrode. Afterward, the electrode was rinsed copiously with ultrapure water.

Electrodes for capillary electrophoresis were sealed in a polypropylene pipet tip (Ultramicro pipet tip 0.5−10 $\mu$L, Daigger, Vernon Hills, IL). The diamond microelectrode was inserted into the pipet tip, and a piece of a heat-shrink tubing (2 mm length, 1.5 mm i.d.) was placed around the end. Heat was applied with a heat gun to soften the underlying polypropylene. The contraction of the heat-shrink tubing served to conform the softened polypropylene coating over the surface. This procedure effectively sealed the cylindrical portion of the electrode, leaving a small conically shaped electrode exposed. Melted polypropylene or epoxy was used to secure the copper wire current collector at the top of the pipet tip.

**Electrochemical Measurements.** Cyclic voltammetry was performed in an ∼8 mL, single compartment glass cell. A three-electrode system consisting of a diamond working electrode, a Ag/AgCl reference electrode, and a carbon rod auxiliary electrode was connected to either a CS-1200 or a CS-1090 potentiostat (both Cypress Systems, Lawrence, KS). The cell was housed in a Faraday cage that was electrically grounded. All measurements were made at room temperature in solutions deoxygenated with $N_2$ for 10 min.

**Capillary Electrophoresis.** Capillary electrophoresis was performed, using a homemade system consisting of a 10- or 30-kV power supply CZE1000R (Spellman, Hauppauge, NY), a homemade timer for electrokinetic injection, and a Plexiglas box with an interlock housing the 30- or 50-cm-long, 75-$\mu$m-i.d. fused-silica capillary (Polymicro Technologies, Phoenix, AZ), buffer reservoir, sample vessel, and a 20-mL detection cell (Figure 1). The box was covered by electrically grounded aluminum foil, which shielded the system from spurious electromagnetic signals. A three-electrode assembly consisting of a diamond working electrode, a Ag/AgCl reference electrode, and a platinum auxiliary electrode was connected to the potentiostat (model 832A, CH Instruments, Austin, TX). New capillaries were activated by flushing sequentially with 0.1 M NaOH, water, 0.1 M HCl, water, and run buffer for 30 min each. Prior to a series of measurements, the capillary was flushed with run buffer.

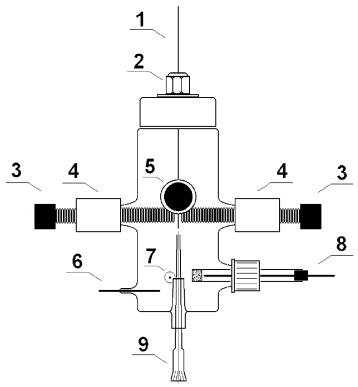


Figure 1. Diagram of the electrochemical detection cell used for capillary electrophoresis: (1) end portion of the separation capillary; (2) chromatography fitting; (3) lower pair of Kel-F bolts for adjusting the capillary position in the *x* direction, (4) Teflon parts with threads; (5) upper pair of Kel-F bolts for adjusting the capillary position in the *y* dimension; (6) platinum wire for high voltage connection; (7) platinum wire attached at the rear part of the cell, which serves as an auxiliary electrode; (8) Ag/AgCl reference electrode; and (9) working boron-doped diamond microelectrode sealed in polypropylene pipet tip.

**Safety Considerations.** The high-voltage power supply and associated electrical connections should be handled with extreme caution to avoid electrical shock.

## RESULTS AND DISCUSSION

**Electrode Characterization.** Figure 2a shows SEM images of sharpened Pt wires (76-, 25-, and 10-$\mu$m diameter labeled 1, 2, and 3, respectively). The wires were etched to a sharp point with a radius of curvature of ∼100 nm (see also Figure 3a). SEM images of wires removed from the reactor after 30 min of deposition at the high methane concentration (3.5% $CH_4/H_2$) showed extensive diamond nucleation. Complete coverage with polycrystalline diamond was achieved after 10 h using a 0.5% $CH_4/H_2$ source-gas ratio. Figure 2b shows SEM images of the sharpened wires conformally coated with diamond. In all cases, the film covers the entire wire with no visible cracks or defects. The films were slowly cooled from the growth temperature to minimize thermal stress due to the difference in thermal expansion coefficients of diamond ($1 \times 10^{-6}$/°C) and platinum ($9 \times 10^{-6}$/°C). Diamond's rough, polycrystalline morphology is apparent from the images in Figures 2b.

The SEM image in Figure 3b reveals that the diamond film is ∼4.5 $\mu$m thick. The radius of curvature for all the electrodes, regardless of the Pt wire diameter, is ∼5 $\mu$m (Figure 3c) because of the diamond film thickness. A film thickness of 1−2 $\mu$m is necessary for growth from all the individual crystallites to coalesce into a continuous film. The films consist of randomly oriented, well-faceted diamond crystallites (Figure 3d) with base diameters from 1 to 3 $\mu$m. However, a wide grain-size distribution exists. The smaller grains located on the larger crystal facets and in the grain boundaries between the larger crystallites are secondary growths of diamond. There is extensive twinning and, in general, these films appear to have more morphological defects than do films deposited on Si substrates when similar conditions are used.

Figure 4 shows Raman spectra of diamond films grown on (a) a sharpened 76 $\mu$m diameter Pt wire and (b) a silicon substrate.

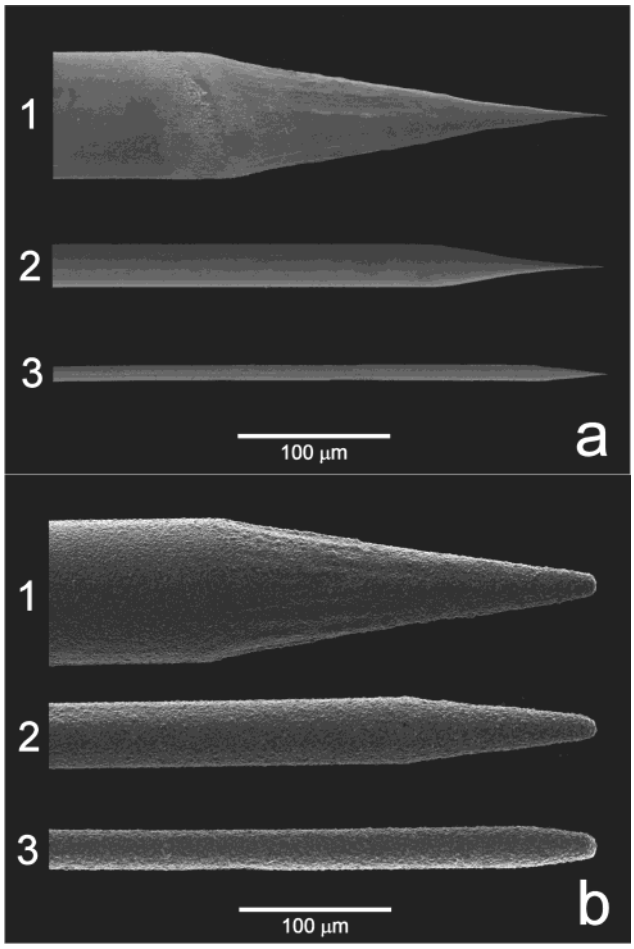


Figure 2. SEM images of (a) electrochemically sharpened platinum wires and (b) platinum wires covered with a polycrystalline boron-doped diamond film. The wires were (1) 76 , (2) 25, and (3) 10 $\mu$m in diameter (magnification of 300×).

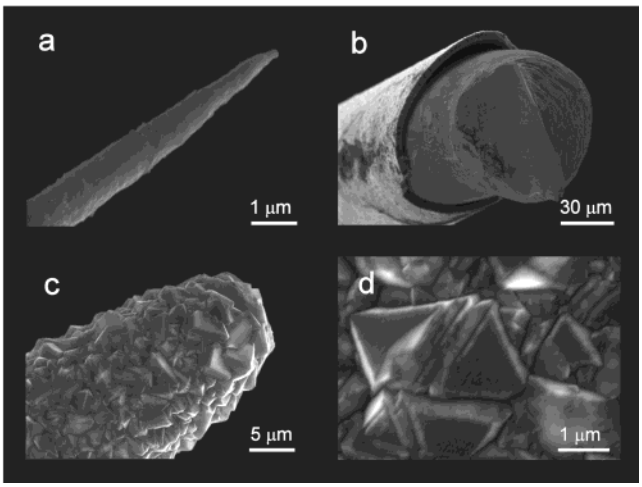


Figure 3. SEM images of (a) the end of a 76-$\mu$m electrochemically etched platinum wire; (b) a cross section of the 76-$\mu$m wire covered with a boron-doped diamond film, obtained by cutting the microelectrode with razor blade; (c) the tip of a 25-$\mu$m Pt wire covered with a boron-doped diamond film; and (d) the surface of the polycrystalline diamond film deposited on the platinum wire.

The deposition conditions were the same for both substrates. Both spectra show an intense one-phonon diamond line at 1333 $cm^{-1}$. The full width at half-maximum (fwhm) of this peak is ~12 $cm^{-1}$ for the film deposited on Pt and ~8 $cm^{-1}$ for the film grown on Si. By comparison, the fwhm for single-crystal diamond is 2 $cm^{-1}$. The larger fwhm for the film deposited on Pt is indicative of a higher defect density because, to a first approximation, the peak width is inversely related to the phonon lifetime (i.e., phonon scattering by grain boundaries and defects).[25] This is consistent with the SEM images that show significant secondary growths and, in general, a high fraction of grain boundary. The broad peak at 1580 $cm^{-1}$ is due to the presence of nondiamond, $sp^2$-bonded carbon impurity, and the peak position suggests that the impurity has some graphitic character. The impurity is located mainly at the interface between the Pt and diamond, and not on the film surface.[25] This was confirmed by examining the background voltammetric response, which showed no evidence for the impurity, and the Raman spectrum for a film before and after acid washing (refluxing for 30 min sequentially in (i) aqua regia and (ii) 30% $H_2O_2$) and hydrogen plasma treatment, a procedure that effectively removes nondiamond carbon impurity from the surface.[8] The Raman spectrum was unaffected by the treatment, consistent with the existence of the impurity at the Pt/diamond interface. The diamond film is sufficiently transparent to the excitation radiation such that scattering intensity from the interface is detected. The production of nondiamond carbon on the Pt surface probably occurs, to a large extent, during the first 30 min of deposition at the high $CH_4/H_2$ ratio of 3.5% used to enhance the nucleation.

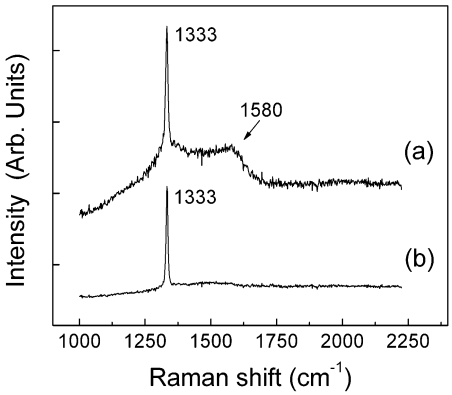


Figure 4. Raman spectra for polycrystalline boron-doped diamond films deposited on (a) a 76-$\mu$m platinum wire and (b) a p-Si (100) substrate.

**Basic Voltammetric Response.** Electrochemical characterization of the diamond microelectrodes, formed on the 76-$\mu$m-diameter Pt, was performed in a microcylinder geometry with an electrode length of ~1.5 mm. The exposed electrode area was nominally $3.5 \times 10^{-3}$ $cm^2$, based on the magnitude of the voltammetric limiting current measured for $Ru(NH_3)_6^{3+/2+}$. However, there was a rather large 20% variability in the exposed area from experiment to experiment. The microelectrodes exhibited a low and stable voltammetric response in 1 M KCl; 0.1 M $HClO_4$; and 0.1 M phosphate buffer, pH 7.4, with a potential window of >2.5 V (±10 $\mu A/cm^2$ geometric). The background current was noticeably smaller at negative than at positive potentials. The electrodes exhibited no characteristic Pt voltammetric features,

(25) Tachibana, T.; Yokota, Y.; Miyata, K.; Onishi, T.; Kobashi, K.; Tarutani, M.; Takai, Y.; Shimizu, R.; Shintani, Y. *Phys. Rev. B* **1997**, *56*, 15967.

Table 1. Summary of Cyclic Voltammetric Peak Potentials, $E_p$, and Half-Peak Potentials, $E_{p/2}$, for Several Redox Analytes at Diamond Microelectrodes[a]

| analyte | $E_p$, mV | $E_{p/2}$, mV |
|---|---|---|
| $Ru(NH_3)_6^{3+/2+}$ | −309 ± 7 | −186 ± 2 |
| $Fe(CN)_6^{3-/4-}$ | 386 ± 23 | 283 ± 2 |
| catechol | 647 ± 24 | 544 ± 8 |
| 4-methylcatechol | 667 ± 20 | 495 ± 6 |
| *tert*-butylcatechol | 578 ± 19 | 443 ± 11 |
| epinephrine | 623 ± 25 | 473 ± 8 |
| norepinephrine | 597 ± 14 | 456 ± 12 |
| dopamine | 576 ± 15 | 421 ± 17 |
| DOPAC | 797 ± 22 | 614 ± 19 |

[a] The values represent an average ± standard deviation from measurement with five different microelectrodes. Analyte concentrations: 1mM in 1 M KCl. Scan rate: 0.1 V/s. The diamond microelectrodes (76-$\mu$m-diameter Pt wire) were used in a microcylinder geometry without any insulation.

indicating the absence of cracks and pinholes. The reproducibility of the voltammetric response shape and current magnitude for $Ru(NH_3)_6^{3+/2+}$, $Fe(CN)_6^{3-/4-}$, the catechols, and the catecholamines (1 mM solutions in 1M KCl) was evaluated using five different microelectrodes. At a scan rate of 0.1 V/s, the electrodes were large enough in radius that they did not exhibit a time-independent or steady-state limiting current. Rather, the electrodes showed mixed macroelectrode/microelectrode cyclic voltammetric behavior with some peak-shaped character on both the forward and reverse sweeps. An important first task in this research project was to evaluate the reproducibility of the diamond deposition and the electrode's voltammetric response. Table 1 presents a summary of the peak potentials, $E_p$, and half-peak potentials, $E_{p/2}$, for several aqueous redox analytes. All values, except those for $Ru(NH_3)_6^{3+/2+}$, are for the oxidation half reaction. Clearly, the diamond microelectrodes yield a reproducible response in terms of peak position. The fact that the exposed area was unknown for each electrode made it difficult to compare the reproducibility of the peak currents.

**Voltammetric Response for Insulated Electrodes.** Several methods were tested for their effectiveness in insulating the cylindrical portion of the 76-$\mu$m-diameter microelectrodes. The reproducibility in application and the effectiveness of the insulating coating were from the voltammetric response for various test analytes. The exposed electrode area was determined from the limiting current measured for $Ru(NH_3)_6^{2+/3+}$. In general, all of the coating methods result in the formation of an electrode with a mixed cylinder and cone geometry. Therefore, the mass transport-limited current, $i_{lim}$, at the diamond microelectrodes is described by a cylindrical and a conical term according to the equation

$$i_{lim} = i_{qss}^{cylinder} + i_{ss}^{cone} \quad (1)$$

For a quasi-steady-state current (long time limit), it holds that the cylindrical term, $i_{qss}^{cylinder}$, is given by[26]

$$i_{qss}^{cylinder} = \frac{2nFADC}{r \ln \tau} \quad (2)$$

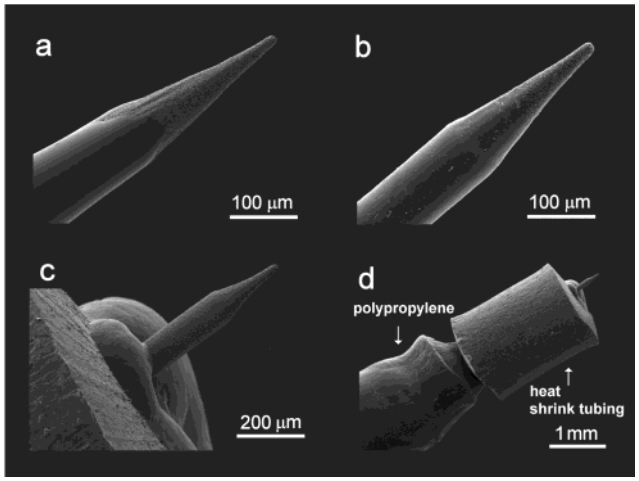


Figure 5. SEM images of a 76-$\mu$m diamond microelectrode insulated with (a) 2 layers of nail polish, (b) 7 layers of polyimide, and (c) polypropylene. Picture d shows a low magnification SEM image of the top part of the diamond microelectrode insulated in a polypropylene pipet tip with a piece of heat-shrink tubing.

and the conical term, $i_{ss}^{cone}$, by[27]

$$i_{ss}^{cone} = 4nFDCr(1 + qH^p) \quad (3)$$

In both equations, $n$ is the number of electrons transferred per equivalent, $F$ is the Faraday constant, $A$ is the electrode area ($cm^2$), $D$ is the diffusion coefficient ($cm^2/s$), $C$ is the bulk concentration of the analyte ($mol/cm^3$), $r$ is the cylinder or cone radius (cm), $\tau = 4Dt/r^2$, $q = 0.30661$, $p = 1.14466$, and $H$ is the aspect ratio $h/r$ where $h$ is height of the cone (cm). The measurement period, $t$ (s), is the time of the forward voltammetric scan. The surface area of a cone is related to its aspect ratio according to the equation $A = \pi r^2(H + 1)^{1/2}$. The theoretical current originating from the cone portion of the microelectrode was calculated using eq 3, with the cone dimensions obtained from SEM images (Figure 2b). When the measured current exceeded the calculated value, a portion of the cylinder was presumed exposed. In this case, the length of the cylindrical part was calculated using eqs 1 and 2, in which $A = 2\pi rl$. When the measured current was smaller than the theoretical value, only a part of the cone was exposed, and its dimension was calculated using eq 3. The exposed microelectrode area was calculated according to the equations describing the limiting currents for hemispherical or disk microelectrodes.[26] For all calculations, diffusion coefficients of $6.7 \times 10^{-6}$ $cm^2$ $s^{-1}$ for $Fe(CN)_6^{-4}$ and $7.0 \times 10^{-6}$ $cm^2$ $s^{-1}$ for $Ru(NH_3)_6^{3+}$, a cone aspect ratio of 6.0, and a time ($t$) of 30 s were used.

SEM images of some insulated diamond microelectrodes are presented in Figure 5. The exposed area, as estimated from the images, compared well with the area determined from the limiting current for $Ru(NH_3)_6^{2+/3+}$. The simplest way to insulate the microelectrode is to coat the surface with nail polish or an epoxy. An example of a microelectrode coated with nail polish is given

(26) Bard, A. J.; Faulkner, L. R. Diffusion Controlled Currents at Ultramicroelectrodes. In *Electrochemical Methods Fundamentals and Applications*, 2nd ed.; John Wiley & Sons: New York, 2001; pp 168−176.
(27) Zoski, C. G.; Mirkin, M. V. *Anal. Chem.* **2002**, *74*, 1986.

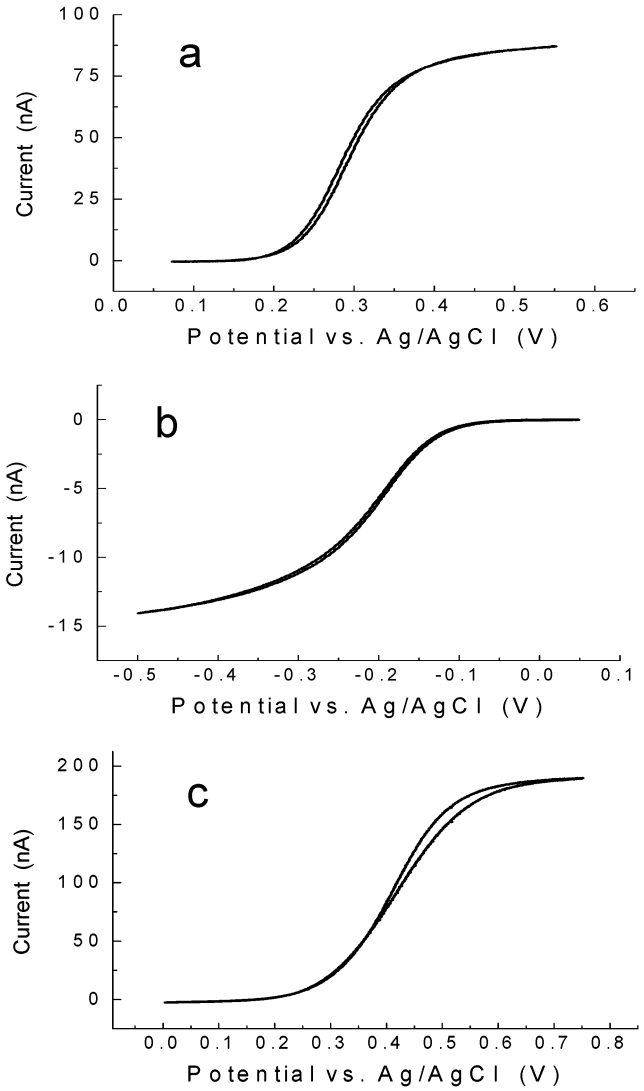


Figure 6. Cyclic voltammetric $i-E$ curves for boron-doped diamond microelectrodes in (a) 1 mM $K_4$ [$Fe(CN)_6$] and 1 M KCl at a nail polish-insulated microelectrode (10 mV/s), (b) 1 mM [$Ru(NH_3)_6$]$Cl_3$ and 1 M KCl at a polyimide-insulated microelectrode (10 mV/s), and (c) 1 mM $K_4$ [$Fe(CN)_6$] plus 1 M KCl at a nail polish-insulated microelectrode (25 mV/s). Curves a and b are for microelectrodes constructed with a 76-$\mu$m-diameter Pt wire and curve c is for a microelectrode constructed with a 25-$\mu$m-diameter Pt wire.

in Figure 5a. It can be seen that the entire cylindrical portion of the electrode is coated, with the coating edge seen where the taper of the wire starts. Two or three layers of nail polish were sufficient to completely insulate the cylindrical portion. The nail polish dries quickly, so the procedure is rapid. Unfortunately, this method does not offer adequate reproducibility, in terms of the exposed area, because it is difficult to coat all the way to the end of the electrode, i.e., to control the amount of the cone that is covered. As a result, the electrodes exhibited steady-state currents reflective of areas ranging from $2 \times 10^{-3}$ to $2 \times 10^{-5}$ cm$^2$. Sigmoidally shaped voltammetric curves were observed for $Ru(NH_3)_6^{3+/2+}$ and $Fe(CN)_6^{3-/4-}$ only at scan rates below 25 mV/s, as shown in Figure 6a. The Tomeš criterion ($E_{3/4} - E_{1/4}$), which is a measure of the steady-state voltammetric curve slope and should be 56/n mV for a reversible redox couple, ranged from 57 to 77 mV. The electrodes with higher Tomeš criteria presumably had a higher internal ohmic resistance due to a lower boron-doping level. Films doped using the solid-state source tend to have a wider range of doping levels (i.e., electrical conductivity) for the same set of deposition conditions than do films doped from a gas-phase source, such as $B_2H_6$. The chemical stability of the nail polish coating is certainly questionable. However, we did not observe any problems with stability in the aqueous solutions tested.

Polyimide coatings were also investigated, as this material should be more chemically inert than the nail polish.[19] Polyimide coatings exhibit exceptional chemical resistance, mechanical toughness, thermal stability, and good dielectric properties. The microelectrodes were first completely covered by dipping the electrodes into the coating solution multiple times and curing in an oven. The polymer layer near the end of the electrode was then removed by dissolution in sodium hydroxide. This was accomplished by placing the electrode end in contact with a Kimwipe saturated with 0.1 M NaOH. A linear dependence was observed between the soak time and the exposed area. The coating did effectively insulate the electrode, but unfortunately, the exposed area after dissolution varied widely from $2 \times 10^{-4}$ to $5 \times 10^{-7}$ cm$^2$. The variability results from the manner in which the polymer dissolution is accomplished. It is difficult to keep solution in contact with just the very end of the electrode. Note that electrodes in the lower part of this range have exposed areas smaller than or comparable to the cross section of a 10-$\mu$m-diameter carbon fiber. An example of the microelectrode insulated with polyimide is presented in Figure 5b. The edge of the smooth polymer coating, which is only several micrometers thick, is difficult to see. Close inspection of the image, however, reveals that the entire cylindrical portion of the electrode, and about one-half of the cone is insulated. Higher resolution SEM images of the exposed end of several electrodes revealed the presence of small polymer deposits between the diamond grains, even after dissolution in NaOH. Apparently, the dissolution is not complete, even after extensive soaking in NaOH.

Another more significant complication with the polyimide coating was the noticeably reduced working potential window at negative potentials. It seems that there is a reduction reaction involving a component in the coating that gives rise to a significant cathodic background current. Therefore, microelectrodes coated with this polymer are useful only for measurements at positive potentials ($> -0.5$ V vs Ag/AgCl), because this region is seemingly unaffected by the coating. Although the curves were stable with scan number, steady-state limiting currents were not obtained (Figure 6b). The reason for this is probably the cathodic current associated with the redox-active component in the coating. The Tomeš criterion varied from 59 to 77 mV, and as in the previous case, the difference from the theoretical value of 56 mV can be attributed to ohmic resistance.

Polypropylene, a versatile polymer with good chemical stability, was also used to insulate the diamond microelectrodes, specifically those applied for CE−EC. Disposable polypropylene pipet tips were used for quick and simple insulation of the microelectrodes formed with 76-$\mu$m-diameter Pt wires. The polypropylene adheres strongly to the diamond surface. Examples of pipet tip-insulated microelectrodes are shown in Figure 5c,d. A piece of heat-shrink tubing was placed around the polypropylene/electrode coating

and used to compress the polymer against the electrode surface when softened during heating (see Figure 5d). There are no cracks formed and no delamination of the polymer around the diamond. The absence of leakage was confirmed by the observation of a stable background current and analyte response during extended use. Sigmoidal voltammetric curves were observed for $Ru(NH_3)_6^{3+/2+}$ and $Fe(CN)_6^{3-/4-}$ at scan rates below 25 mV/s. The polypropylene-insulated electrodes had surface areas in the range $2 \times 10^{-3}$ to $3 \times 10^{-5}$ cm$^2$. Fabrication of electrodes with a small exposed area is difficult using this method; therefore, a small amount of nail polish was sometimes used to reduce the exposed area. Such electrodes were used for analysis in aqueous media only. The Tomeš criteria for the test analytes were in the same range as those observed for the nail polish-insulated electrodes.

The voltammetric response of the diamond microlectrodes with smaller diameters (25- and 10-$\mu$m diameters) was also investigated. The electrodes were insulated with nail polish, and their properties were evaluated using $Ru(NH_3)_6^{3+/2+}$ and $Fe(CN)_6^{3-/4-}$. The electrodes gave sigmoidally shaped voltammetric curves with little hysteresis for both analytes at low scan rates (<25 mV/s). An example of a cyclic voltametric $i-E$ curve for $Ru(NH_3)_6^{3+/2+}$, recorded with a 25-$\mu$m-diameter electrode, is presented in Figure 6c. The response (half-wave potential and Tomeš criterion) variability for the smaller diameter electrodes was generally greater than for the 76-$\mu$m-diameter electrodes. This is due to the fact that the very narrow wires easily flex when mounted in the deposition chamber. This leads to a thermal gradient across the wire substrate during diamond deposition. The uneven heating causes the deposition of lower quality diamond containing a mixture of $sp^3$- and $sp^2$-bonded carbon. As a result, diamond films with less reproducible electrochemical properties are produced. Nonetheless, electrodes of these dimensions can also be used for the measurements.

**Capillary Electrophoresis.** A simple electrochemical detection cell was designed to investigate the diamond microelectrode performance in CE−EC (see Figure 1). Diamond films coated on the 76-$\mu$m-diameter Pt wires, insulated in polypropylene pipet tips, were employed for amperometric detection. Decoupling the separation voltage from the electrode signal was accomplished by an end-column arrangement with the diamond microelectrode positioned just outside the end of the capillary column. The distance between the capillary and the microelectrode was adjusted (eyesight) by moving the capillary, which was mounted in the detection cell normal to the working electrode. The alignment of the capillary in the $x-y$ plane, with respect to the microelectrode, was adjusted using two pairs of Kel-F bolts.

Basic characterization of the CE−EC system was performed using a 10 mM phosphate buffer, pH 6.0, (deoxygenated with $N_2$) run buffer, a 30-cm-long separation capillary (75-$\mu$m i.d.), and a separation voltage of 8 kV (267 V/cm). Solutes were injected electrokinetically for 3 s at 8 kV. The diamond working electrode had an approximate exposed area of $9.8 \times 10^{-4}$ cm$^2$. The background current and peak-to-peak noise, as a function of the applied potential, were measured between −0.6 and +1.4 V vs Ag/AgCl. The working electrode was manually aligned close to the end of the fused-silica capillary, and the separation voltage was then switched on. Following this, the detection potential was applied, with the background current quickly stabilizing (often in less than 3 min). The background was measured after 20 min at a given potential, and the peak-to-peak noise was averaged from 4 to 6 readings. The results, shown in Figure 7, indicate low background current of ∼100 pA and noise of ∼3 pA at potentials from 0 to 1.3 V. The background current for a diamond microelectrode ($9.8 \times 10^{-4}$ cm$^2$) was a factor of 5−10 lower at the detection potential than the background current for a carbon fiber microelectrode ($7.9 \times 10^{-4}$ cm$^2$).

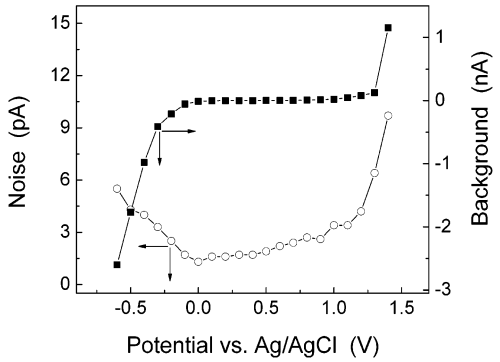


Figure 7. Diamond microelectrode noise (○) and background current (■) measured in 10 mM phosphate buffer, pH 6.0, (separation voltage of 8 kV) (76-$\mu$m-diameter Pt) at different detection potentials.

The decoupling of the separation voltage was next investigated. Cyclic voltammograms of catechol (0.1 mM in 10 mM phosphate buffer, pH 6.0) were recorded in the CE detection cell, while the separation voltage applied was varied from 0 to 20 kV. Run buffer flowed through the column during the measurements. A scan rate of 0.1 V/s was used so that peak-shaped curves were obtained. With this arrangement, complete electrical isolation of the electrode signal was not achieved. The peak current was independent of the separation voltage, but the oxidation peak potential shifted positive with increasing separation voltage. In fact, a linear dependence ($R = 0.995$) between the separation voltage and the oxidation peak potential for catechol was found. For example, a separation voltage of 8 kV resulted in the peak shift of ∼45 mV in one experiment. Therefore, complete decoupling of the high voltage was not achieved in our arrangement, in part, because of the relatively wide capillary used (75-$\mu$m i.d.) and the close positioning of the working electrode. Improved decoupling should be achieved by decreasing the column diameter. Experiments are currently in progress to test this supposition.

Hydrodynamic voltammograms (HDVs) for dopamine and catechol were recorded to determine the optimum detection potential. Figure 8 shows examples of HDVs for 10 $\mu$M catechol and dopamine. Each point represents the average of three measurements. The maximum S/N ratio was achieved at 1.1 V vs Ag/AgCl, and this potential was chosen for detection. Again, this potential is shifted positive by ∼45 mV from where it would be otherwise as a result of the incomplete decoupling of the separation voltage.

Figure 9 shows an example electropherogram, albeit with relatively low efficiency, for dopamine, catechol, and ascorbic acid. The separation was conducted in a 30-cm column (75-$\mu$m i.d.) at 8 kV. The run buffer was 10 mM phosphate buffer, pH 6.0. At this pH, dopamine is a cation, catechol is neutral, and ascorbic acid is an anion. All three solutes are well-resolved. The differences in the peak height can be explained by the different migration

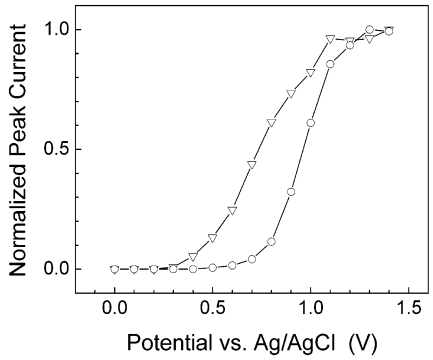


Figure 8. Hydrodynamic voltammograms for dopamine (▽) and catechol (○) measured in 10 mM phosphate buffer, pH 6.0, at a diamond microelectrode (76-$\mu$m-diameter Pt). Electrokinetic injection for 3 s at 8 kV. Capillary length = 30 cm (75-$\mu$m i.d.). Separation voltage = 8 kV. Analyte concentration = 10 $\mu$M.

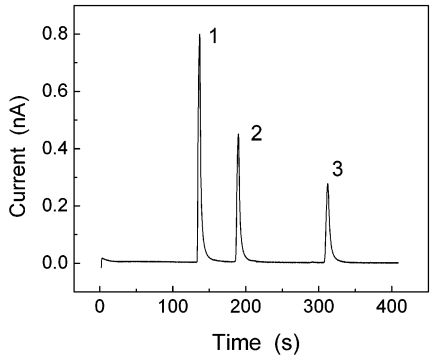


Figure 9. Electropherogram for a mixture of dopamine (1), catechol (2), and ascorbic acid (3) in 10 mM phosphate buffer pH 6.0. Detection was made with a diamond microelectrode (76-$\mu$m-diameter Pt). Electrokinetic injection for 3 s at 8 kV. Capillary length = 30 cm (75-$\mu$m i.d.). Separation voltage = 8 kV. Detection potential = +1.1 V vs Ag/AgCl. The dopamine and catechol concentrations were 5 $\mu$M, and the ascorbic acid concentration was 10 $\mu$M.

rate for each analyte (highest rate for the cationic dopamine and the lowest rate for the anionic ascorbic acid) during the electrokinetic injection. Note that ascorbic acid concentration is two times higher than that for dopamine and catechol. The injected volume, calculated from the migration time of catechol, a neutral species at pH 6.0, was estimated to be 21 nL. The nominal retention times (three injections) for the three solutes were 136.5 ± 0.130, 189.4 ± 0.133, and 311.5 ± 0.140 s, respectively. The peak widths at half-height were 3.23 ± 1.78, 3.46 ± 1.67, and 4.27 ± 1.35 s, respectively. Relative standard deviations are presented for both sets of data. The separation efficiencies were ~33 000, 56 000, and 98 000 plates/m ($N = 5.54(t_m^2/w_{1/2}^2)$). These separation efficiencies are rather low as compared to what is normally observed in CE. This is because of the low separation voltage, 8 kV; the short column, 30 cm; and the large column inner diameter, 75 $\mu$m. Even though the efficiency was low, the results demonstrate that the separation and detection are very reproducibile.

Table 2 presents a summary of the detection figures of merit for dopamine and catechol. The reproducibility of the electrode response was determined from 15 consecutive injections of a mixture of dopamine and catechol (5 $\mu$M each prepared in the run buffer). Good reproducibility in terms of the peak height and area is observed, with a variance (relative standard deviation) of 4.1% or less for both analytes. The linear dynamic range is 3−4

Table 2. CE−EC Detection Figures of Merit for Dopamine and Catechol[a]

| parameter | dopamine | catechol |
|---|---|---|
| peak height repeatability, % | 3.0 | 4.0 |
| peak area repeatability, % | 2.6 | 4.1 |
| peak width $w_{h/2}$, s | 3.6 ± 0.2 | 3.7 ± 0.2 |
| linear dynamic range, mol/L | $8 \times 10^{-8}$−$1 \times 10^{-4}$ | $1 \times 10^{-7}$−$1 \times 10^{-4}$ |
| sensitivity (slope), mA L mol$^{-1}$ | 129.7 | 85.2 |
| corr coeff | 0.9997 | 0.9979 |
| concn LOD, mol/L | $7.8 \times 10^{-8}$ | $1.2 \times 10^{-7}$ |
| mass LOD, fmol | 1.7 | 2.6 |

[a] CE−EC parameters were electrokinetic injection for 3 s at 8 kV; capillary length, 30 cm; separation voltage, 8 kV; and detection potential, +1.1 V vs Ag/AgCl. Repeatability of the analyte response was evaluated from 15 consecutive injections of 10 $\mu$M analyte solutions in the run buffer.

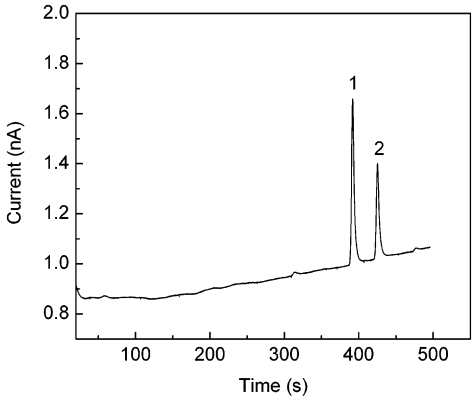


Figure 10. Electropherogram of a 2-naphthol (1) and 1-naphthol (2) mixture in 160 mM borate buffer, pH 9.2. Electrokinetic injection for 4 s at 7 kV. Capillary length = 51 cm. Column diameter = 75 $\mu$m. Separation voltage = 12 kV. Detection potential = 1.0 V vs Ag/AgCl. The naphthol concentrations were 10 $\mu$M each.

orders of magnitude for both analytes. At high concentrations (>0.1 mM), the response curve exhibited rollover due to column overloading. Plots of peak area versus solution concentration yielded the widest dynamic range, with correlation coefficients of 0.9994 and 0.9993 for dopamine and catechol, respectively. The limit of detection, calculated for S/N = 3 and noise of 3.4 pA, was 78 nM (1.7 fmol) for dopamine and 120 nM (2.6 fmol) for catechol. Although we have not yet performed a detailed comparison of the diamond electrode performance with that of other commonly used electrodes (e.g., carbon fibers), the figures of merit compare favorably with those reported for carbon fiber and diamond microelectrodes.[7,15,28] The diamond microelectrodes exhibited good performance. They provided a stable and reproducible response for the redox test analytes, with no evidence of any electrode deactivation during extended use. Additionally, no pretreatment was required to activate the electrode initially.

Figure 10 shows an electropherogram for a mixture of 10 $\mu$M 1- and 2-naphthol. The run buffer was 160 mM borate buffer, pH 9.2, in a 51-cm (75-$\mu$m-diameter) fused-silica column. At this pH, both solutes are deprotonated and anionically charged. The separation voltage was 12 kV, and the detection potential was 1.0

(28) Woods, L. A.; Roddy, T. P.; Paxon, T. L.; Ewing, A. G. *Anal. Chem.* **2001**, *73*, 3687.

V vs Ag/AgCl. Electrokinetic injection was used at 7 kV for 4 s. The migration times are 391.7 and 425.2 s, respectively, for 2- and 1-naphthol. Much higher efficiency is seen for this separation, as compared to the one for the three analytes discussed above, with theoretical plate numbers of 118 000 and 126 000 plates/m, respectively.

## CONCLUSIONS

Sharpened platinum wires are a suitable substrate for the deposition of boron-doped polycrystalline diamond films to form microelectrodes useful for electroanalytical measurements. Microelectrodes with a combined conical and cylindrical shape that exhibit reproducible voltammetric responses, at least in terms of the peak and half-wave potentials, for a variety of aqueous redox analytes can be fabricated. The voltammetric response is affected by boron-doping level (ohmic resistance) and the shape of the electrode. Several methods were evaluated for their ability to insulate the cylindrical portion of the microelectrode, reproducibly exposing a disk geometry at the end, including polyimide, nail polish, epoxy, and polypropylene coatings. Although all of the coatings appear to adhere strongly to the diamond surface, the limited chemical or electrochemical stability of some (e.g., nail polish and polyimide) restrict their use to certain environments and potential ranges. More importantly, there is still too much variability in the exposed electrode area for any of these coating methods. Polypropylene pipet tips were found to be a suitable insulation material for the microelectrodes used in CE−EC. Two sets of solutes were separated electrophoretically: (i) dopamine, catechol, and ascorbic acid and (ii) 1- and 2-naphthol. Efficient separation of these analytes, with reproducible retention times and peak widths, were observed. The results demonstrate that diamond microelectrodes are a useful new electrode material for electrochemical detection in capillary electrophoresis. Diamond microelectrodes, without any activation pretreatment, exhibited low background current (~100 pA) and noise (e.g., 3 pA), even at an anodic detection potential of 1.1 V vs Ag/AgCl, reproducible responsiveness for various analytes with response precisions <4%, a wide linear dynamic range of ~4 orders of magnitude, and limits of detection ($S/N = 3$) of 1.7 and 2.6 fmol, for dopamine and catechol, respectively.

Future research will involve (i) depositing diamond films on Pt substrates doped using a gas-phase source ($B_2H_6$), which should yield higher and more reproducible electrode conductivities; (ii) redesign of the electrode holder and detection cell in order to gain better control over the working electrode−column separation distance and more complete decoupling of the separation voltage; and (iii) continued efforts to develop a protocol for insulating the cylindrical portion of the electrode and reproducibly exposing the end.

## ACKNOWLEDGMENT

J. Cvačka gratefully acknowledges NATO Science Fellowship Program 2001/2002 for support of his visit at Michigan State University. V. Quaiserová gratefully acknowledges The Mobility Fund of Charles University and Hlávka's Foundation for support of her visit at Michigan State University. This research was supported by the National Institutes of Health (GM 65958-01) and the National Science Foundation (CHE-0049090). The authors thank Vada O'Donnell for her assistance in preparing this manuscript.

Received for review January 9, 2003. Accepted March 24, 2003.

AC030024Z